

Nonlinear Formation Control of Marine Craft with Experimental Results

Ivar-André F. Ihle¹, Roger Skjetne^{1,2} and Thor I. Fossen^{1,2}

Abstract—Decentralized formation control schemes for a fleet of vessels with a small amount of intervessel communication are proposed and investigated. The control objective for each vessel is to maintain its position in the formation relative to a Formation Reference Point, which follows a predefined path. This is done by constructing an individual parameterized path for each vessel so that when the parametrization variables are synchronized, the vessels are in formation. To obtain this, an individual maneuvering problem is solved for each vessel, with an extension of a synchronization feedback function in the dynamic control laws to ensure that the vessels stay assembled in the desired formation. This setup assures that all vessels will have the same priority, i.e. no leader. Performance and theoretical results are validated by experiments for a scaled model ship and a computer simulated ship in a marine control laboratory.

I. INTRODUCTION

The topic of this paper is formation control of ships using a control design concept that requires only a small amount of intervessel communication. The design procedure is based on the *maneuvering control design* proposed in [1] and [2]. Briefly explained, the maneuvering design is based on separating the desired behavior of the system in the output space into two subproblems, the *Geometric Task* and the *Dynamic Task*. The former is to *converge to*, and *follow* a desired parameterized path, and the latter is to *satisfy a desired speed assignment* along the path.

The field of formation control with applications towards mechanical systems such as ships, autonomous underwater vehicles, aircraft, etc., has been widely discussed. The cooperation between members in a formation requires the exchange of signals, and this leads to design considerations such as available communication bandwidth, environmental disturbances, etc. The question of centralized or decentralized control, and communication requirements have been discussed in [3] and references therein. In general, centralized control will require a multidirectional flow of state measurements, sensory information, and necessary guidance signals between each vessel. In environments with restrictive communication options [4, Table 1] such requirements may not be feasible. In decentralized control each system in the formation will have a separate controller under the management of a formation guidance system, and

this can significantly reduce the number of signals being communicated.

In [5], the formation control problem is solved by introducing a *formation reference point* (FRP) and designating each vessel a position relative to that point. Using the maneuvering design, the Geometric and the Dynamic Task ensures that the FRP converges to and follows a desired path $\xi(\theta)$ with a specified speed, where θ is the path parametrization variable. The desired motion of the FRP is based on the states of all the vessels in the formation. The drawback here is the *centralized update law* for $\dot{\theta}$ which needs full state information from all vessels in the formation. Hence, for r vessels, each with n states, the number of communicated signals is $rn + 1$. In order to reduce the signal flow, the formation control problem was solved as a *decentralized scheme* in [6] by solving an individual maneuvering problem for each vessel with an individual path variable θ_i . Then, by synchronizing all the θ_i , $i = 1, 2, \dots$ the formation, represented by the FRP, will move along the path ξ with the desired speed.

In this paper, some theoretical improvements are made to the formation control design in [6]. The most important contribution, however, is the experimental validation for formation control described in the last section of the paper. The formation objective in the experimental activity was a rendezvous operation between two vessels, carried out on a scaled model ship and a computer simulated ship.

Notation: Abbreviations like GS, LAS, UGAS, UGES etc, are U for Uniform, G for Global, L for Local, A for Asymptotically, E for Exponential and S for Stable. A superscript denotes partial differentiation: $f^x(x, y) := \frac{\partial f}{\partial x}$, $f^{x^2}(x, y) := \frac{\partial^2 f}{\partial x^2}$, where the gradient f^x is a row vector. The Euclidean vector norm is $|x| := (x^\top x)^{1/2}$, the distance to the set \mathcal{M} is $|x|_{\mathcal{M}} := \inf_{y \in \mathcal{M}} |x - y|$, and the induced matrix 2-norm of $A \in \mathbb{R}^{n \times n}$ is denoted $\|A\|$. $|(x, y, z)|$ indicates the norm of the vector $[x^\top, y^\top, z^\top]^\top$. For a matrix $P = P^\top > 0$, let $p_m := \lambda_{\min}(P)$ and $p_M := \lambda_{\max}(P)$.

A. Background: Formation setup for ships

A formation of n vessels have n individual paths. We can generalize the setup of a single path ξ to n paths by introducing a Formation Reference Point and create a set of n designation vectors l_i relative to the FRP. Let the FRP be the origin of a moving path frame $\{p\}$ and denote the earth fixed frame $\{e\}$. The desired path for the FRP is $\xi(\theta)$, and

This project is sponsored by the Centre for Ships and Ocean Structures (CESOS), Norwegian Centre of Excellence at NTNU.

¹Centre for Ships and Ocean Structures, Norwegian University of Science and Technology, NO-7491 Trondheim, Norway.

²Department of Engineering Cybernetics, Norwegian University of Science and Technology, NO-7491 Trondheim, Norway.

E-mails: ihle@ntnu.no, skjetne@ieec.org, fossen@ieec.org.

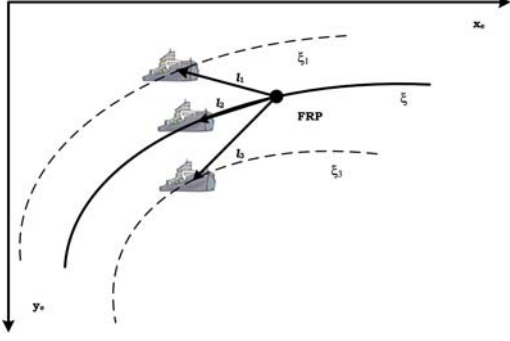


Fig. 1. Formation Setup

Vessel i will then follow the individual desired path

$$\xi_i(\theta_i) = \xi(\theta_i) + R_p^e(\theta_i) l_i, \quad (1)$$

where $R_p^e(\theta_i)$ is a rotation matrix from $\{p\}$ to $\{e\}$. For a vessel on the ocean surface, the output is $\eta = [x, y, \psi]^\top$ where (x, y) is the position and ψ is the heading. The desired path for each vessel is then given by $\xi_i(\theta_i) = [x_{id}(\theta_i), y_{id}(\theta_i), \psi_{id}(\theta_i)]^\top$. The paths are parameterized so that when the path variables are synchronized, the vessels will be in their desired positions relative to the others, see Fig. 1. The tangent vector along the path is chosen as the x -axis of the moving frame $\{p\}$, that is $T(\theta_i) = [x_d^{\theta_i}(\theta_i), y_d^{\theta_i}(\theta_i)]^\top$. The desired heading can then be computed as the angle of the tangent vector in the $\{e\}$ frame

$$\psi_d(\theta_i) = \arctan\left(\frac{T_y(\theta_i)}{T_x(\theta_i)}\right) = \arctan\left(\frac{y_d^{\theta_i}(\theta_i)}{x_d^{\theta_i}(\theta_i)}\right), \quad (2)$$

where $x_d(\theta_i)$ and $y_d(\theta_i)$ are three times differentiable with respect to θ_i . The rotation matrix $R_p^e(\theta_i) = R(\psi_d(\theta_i))$ for the vessels is given by

$$R(\psi_d(\theta_i)) := \begin{bmatrix} \cos \psi_d(\theta_i) & -\sin \psi_d(\theta_i) & 0 \\ \sin \psi_d(\theta_i) & \cos \psi_d(\theta_i) & 0 \\ 0 & 0 & 1 \end{bmatrix}.$$

II. FORMATION CONTROL DESIGN

A general mechanical system is represented by the vector relative degree two model

$$\begin{aligned} \dot{x}_{1i} &= G_{1i}(x_{1i})x_{2i} + f_{1i}(x_{1i}) \\ \dot{x}_{2i} &= G_{2i}(x_{2i})u_i + f_{2i}(x_i) \\ y_i &= h_i(x_{1i}) \end{aligned} \quad (3)$$

where the subscript i denotes the i 'th system. $x_{ji} \in \mathbb{R}^m$ are the states, x_i denotes the full state vector $x_i := [x_{1i}^\top, x_{2i}^\top]^\top \in \mathbb{R}^n$ where $n = 2m$, $y_i \in \mathbb{R}^m$ are the system outputs and u_i are the controls.

The overall control objective is to solve a *Formation Manuevering Problem* (FMP) [5] for r vessels. The geometric task ensures that the individual vessels converge to and stay at their designation in the formation. The dynamic

task ensures that the formation maintains a speed along the path according to the given speed assignment. The paths and speed assignments for the individual vessels are $\xi_i(\theta_i)$, according to (1), and $v_i(\theta_i, t)$, respectively. By construction the paths are parameterized so that $\theta_1 = \theta_2 = \dots = \theta_r$ implies that all vessels are in formation. We assume that the path and speed assignment signals $\xi_i(\theta)$, $\xi_i^\theta(\theta)$, $\xi_i^{\theta^2}(\theta)$ and $v_i(\theta_i, t)$, $v_i^\theta(\theta_i, t)$, $v_i^t(\theta_i, t)$ are uniformly bounded, and the functions G_{1i} , G_{2i} , f_{1i} , and f_{2i} are smooth, and the matrices G_{1i} , G_{2i} , $h_i^{x_{1i}}$ are invertible.

The control design follows a recursive backstepping design described in [1] and [5] where an individual manuevering design is performed for each vessel.

Step 1: The error variables are defined as

$$z_{1i} = z_{1i}(x_{1i}, \theta_i) := y_i - \xi_i(\theta_i) \quad (4)$$

$$z_{2i} = z_{2i}(x_{1i}, x_{2i}, \theta_i, t) := x_{2i} - \alpha_{1i} \quad (5)$$

$$\omega_i := v_i(\theta_i, t) - \dot{\theta}_i, \quad (6)$$

where α_{1i} are virtual controls to be specified later. Differentiating (4) with respect to time gives

$$\begin{aligned} \dot{z}_{1i} &= \dot{y}_i - \xi_i^{\theta_i} \dot{\theta}_i \\ &= h_i^{x_{1i}} G_{1i} z_{2i} + h_i^{x_{1i}} G_{1i} \alpha_{1i} + h_i^{x_{1i}} f_{1i} - \xi_i^{\theta_i} \dot{\theta}_i. \end{aligned}$$

Choose Hurwitz design matrices A_{1i} , so that $P_{1i} = P_{1i}^\top > 0$ are the solutions of $P_{1i} A_{1i} + A_{1i}^\top P_{1i} = -Q_{1i}$ where $Q_{1i} = Q_{1i}^\top > 0$. Define the Step 1 control Lyapunov function (CLF)

$$V_{1i}(x_{1i}, \theta_i) := z_{1i}^\top(x_{1i}, \theta_i) P_{1i} z_{1i}(x_{1i}, \theta_i),$$

whose time derivative becomes

$$\begin{aligned} \dot{V}_{1i} &= 2z_{1i}^\top P_{1i} \left[h_i^{x_{1i}} G_{1i} \alpha_{1i} + h_i^{x_{1i}} f_{1i} - \xi_i^{\theta_i} v_i \right] \\ &\quad + 2z_{1i}^\top P_{1i} h_i^{x_{1i}} G_{1i} z_{2i} + 2z_{1i}^\top P_{1i} \xi_i^{\theta_i} \omega_i. \end{aligned}$$

The first virtual controls are chosen as

$$\begin{aligned} \alpha_{1i} &= \alpha_{1i}(x_{1i}, \theta_i, t) = \\ &G_{1i}^{-1} (h_i^{x_{1i}})^{-1} \left[A_{1i} z_{1i} - h_i^{x_{1i}} f_{1i} + \xi_i^{\theta_i}(\theta_i) v_i(\theta_i, t) \right]. \end{aligned}$$

Define the first tuning function, $\tau_{1i} \in \mathbb{R}$, as

$$\tau_{1i}(x_{1i}, \theta_i) := 2z_{1i}^\top P_{1i} \xi_i^{\theta_i}.$$

Then, the derivative \dot{V}_{1i} becomes

$$\dot{V}_{1i} \leq -z_{1i}^\top Q_{1i} z_{1i} + 2z_{1i}^\top P_{1i} h_i^{x_{1i}} G_{1i} z_{2i} + \tau_{1i} \omega_i.$$

In aid of the next step, we differentiate α_{1i} w.r.t. time to get

$$\dot{\alpha}_{1i} = \sigma_{1i} + \alpha_{1i}^\theta \dot{\theta}_i,$$

where σ_{1i} collects all terms in $\dot{\alpha}_{1i}$ not containing $\dot{\theta}$:

$$\sigma_{1i} := \alpha_{1i}^{x_{1i}} [G_{1i}(x_{1i})x_{2i} + f_{1i}(x_{1i})] + \alpha_{1i}^t(x_{1i}, \theta_i, t).$$

Step 2: Differentiating (5) with respect to time gives

$$\dot{z}_{2i} = \dot{x}_{2i} - \dot{\alpha}_{1i} = G_{2i} u_i + f_{2i} - \sigma_{1i} - \alpha_{1i}^{\theta_i} \dot{\theta}_i$$

Again, choose Hurwitz design matrices A_{2i} , so that $P_{2i} = P_{2i}^\top > 0$ are the solutions of $P_{2i}A_{2i} + A_{2i}^\top P_{2i} = -Q_{2i}$ where $Q_{2i} = Q_{2i}^\top > 0$, and define

$$V_{2i}(x_1, \theta) := V_{1i} + z_{2i}(x_2, \theta_i)^\top P_{2i} z_{2i}(x_2, \theta_i)$$

whose time derivative becomes

$$\begin{aligned} \dot{V}_{2i} &= -z_{1i}^\top Q_{1i} z_{1i} + 2z_{1i}^\top P_{1i} h^{x_{1i}} G_{1i} z_{2i} + \tau_{1i} \omega_i \\ &\quad + z_{2i}^\top P_{2i} \left[G_{2i} u_i + f_{2i} - \sigma_{1i} - \alpha_{1i}^{\theta_i} \dot{\theta}_i \right]. \end{aligned}$$

This results in the control law

$$\begin{aligned} u_i &= \alpha_{2i}(x_i, \theta_i, t) = G_{2i}^{-1} [A_{2i} z_{2i} \\ &\quad - P_{2i}^{-1} G_{1i}^\top (h^{x_{1i}})^\top P_{1i} z_{1i} - f_{2i} + \sigma_{1i} + \alpha_{1i}^{\theta_i} v_i], \end{aligned} \quad (7)$$

and the closed-loop system

$$\begin{aligned} \dot{z}_i &= F_i z_i + g_i \omega_i \\ F_i &= \begin{bmatrix} A_{1i} & h^{x_{1i}} G_{1i} \\ -P_{2i}^{-1} G_{1i}^\top (h^{x_{1i}})^\top P_{1i} & A_{2i} \end{bmatrix} \\ g_i &= \begin{bmatrix} \xi_i^{\theta_i} \\ \alpha_i^{\theta_i} \end{bmatrix}, \end{aligned}$$

where $z_i := [z_{1i}^\top, z_{2i}^\top]^\top$. By defining $P_i := \text{diag}(P_{1i}, P_{2i})$, $Q_i := \text{diag}(Q_{1i}, Q_{2i})$, and the final tuning functions, $\tau_i \in \mathbb{R}$, as

$$\tau_i(x_i, \theta_i) := \tau_{1i} + 2z_{2i}^\top P_{2i} \alpha_{1i}^{\theta_i},$$

the corresponding CLFs with time derivatives become

$$V_i = z_i^\top P_i z_i \quad (8)$$

$$\dot{V}_i \leq -z_i^\top Q_i z_i + \tau_i \omega_i. \quad (9)$$

While (7) defines the static part of the control laws, the dynamic part in traditional maneuvering design for single ships [2] would now proceed by designing an update law for ω_i to render the term $\tau_i \omega_i$ nonpositive, such that the speed assignments are satisfied. For the formation maneuvering problem, however, it is now necessary to ensure both synchronization of the θ_i variables as well as satisfying the speed assignments.

For a cleaner presentation, we collect all states and functions into vector notation. Define the vectors $x := [x_1^\top, \dots, x_r^\top]^\top \in \mathbb{R}^{rn}$, $z := [z_1^\top, \dots, z_r^\top]^\top \in \mathbb{R}^{rn}$, $\theta := [\theta_1, \dots, \theta_r]^\top \in \mathbb{R}^r$, $\omega := [\omega_1, \dots, \omega_r]^\top \in \mathbb{R}^r$, $\tau(x, \theta, t) := [\tau_1, \dots, \tau_r] \in \mathbb{R}^{1 \times r}$, the composite path vector $\xi(\theta) := [\xi_1(\theta_1)^\top, \dots, \xi_r(\theta_r)^\top]^\top \in \mathbb{R}^{rm}$ and the composite speed assignment vector $v(\theta, t) := [v_1(\theta_1, t), \dots, v_r(\theta_r, t)]^\top$. Also, define the matrices $F := \text{diag}(F_1, \dots, F_r)$, $G := \text{diag}(G_1, \dots, G_r)$, $P := \text{diag}(P_1, \dots, P_r)$ and $Q = \text{diag}(Q_1, \dots, Q_r)$. The closed-loop including all vessels is then

$$\begin{aligned} \dot{z} &= Fz + G\omega \\ \dot{\theta} &= v(\theta, t) - \omega, \end{aligned}$$

where $\omega = \omega(x, \theta, t)$ is not yet determined. Let the composite CLF be $V(x, \theta, t) := V_1(x_1, \theta_1, t) + \dots +$

$V_r(x_r, \theta_r, t)$ so that

$$\begin{aligned} V(x, \theta, t) &= z(\theta, t)^\top Pz(\theta, t) \\ \dot{V} &\leq -z^\top Qz + \tau(x, \theta, t) \omega(x, \theta, t). \end{aligned}$$

It can be shown that

$$\tau(x, \theta, t) = -\frac{\partial V}{\partial \theta}(x, \theta, t) = -V^\theta(x, \theta, t),$$

to give

$$\dot{V} \leq -z^\top Qz - V^\theta(x, \theta, t) \omega(x, \theta, t), \quad (10)$$

where $V^\theta(x, \theta, t) = [V_1^{\theta_1}(x_1, \theta_1, t), \dots, V_r^{\theta_r}(x_r, \theta_r, t)]$.

To make sure that the θ_i variables will be synchronized, we introduce the *synchronization constraint function* for θ as

$$\begin{aligned} \Phi_p &: \mathbb{R}^r \rightarrow \mathbb{R}^{r-1}, p \geq 1 \\ \Phi_p(\theta) &= \begin{bmatrix} \phi_1(\theta) \\ \phi_2(\theta) \\ \vdots \\ \phi_{r-1}(\theta) \end{bmatrix} = \begin{bmatrix} (\theta_1 - \theta_2)^p \\ (\theta_2 - \theta_3)^p \\ \vdots \\ (\theta_{r-1} - \theta_r)^p \end{bmatrix}, \end{aligned}$$

where p is a power on the weight. The synchronization constraint function has the Jacobian $\Phi_p^\theta \in \mathbb{R}^{r-1 \times r}$

$$\Phi_p^\theta(\theta) = \begin{bmatrix} \phi_1^{\theta_1} & \phi_1^{\theta_2} & 0 & \dots & 0 \\ 0 & \phi_2^{\theta_2} & \phi_2^{\theta_3} & \dots & 0 \\ \vdots & \vdots & \vdots & \ddots & \vdots \\ 0 & 0 & 0 & \dots & \phi_{r-1}^{\theta_{r-1}} & \phi_{r-1}^{\theta_r} \end{bmatrix}.$$

Notice that the null-space of Φ_p^θ has dimension 1 and is given by

$$\mathcal{N}(\Phi_p^\theta(\theta)) = \left\{ n \in \mathbb{R}^r : n = k [1, \dots, 1]^\top, k \in \mathbb{R} \right\}. \quad (11)$$

The formation maneuvering problem can now be properly stated as rendering the set

$$\mathcal{M} = \{(z, \theta, t) : z = 0, \Phi_p(\theta) = 0\}$$

UGAS under the additional requirement that $(z, \theta, t) \in \mathcal{M} \Rightarrow \omega = 0$ so that the speed assignment is satisfied in \mathcal{M} . Synchronizing $\theta_1 = \dots = \theta_r$ is equivalent to the constraint $\Phi_p(\theta) = 0$. Define the *synchronization CLF*

$$V_s(x, \theta, t) = V(x, \theta, t) + \frac{1}{2} \Phi_p(\theta)^\top \Lambda \Phi_p(\theta) \quad (12)$$

where $\Lambda = \Lambda^\top > 0$ is a weight matrix. The time-derivative of V_s is

$$\begin{aligned} \dot{V}_s &= \dot{V} + \Phi_p(\theta)^\top \Lambda \Phi_p^\theta \dot{\theta} \\ &\leq -z^\top Qz - V^\theta(x, \theta, t) \omega(x, \theta, t) \\ &\quad + \Phi_p(\theta)^\top \Lambda \Phi_p^\theta (v(\theta, t) - \omega) \\ &= -z^\top Qz + \Phi_p(\theta)^\top \Lambda \Phi_p^\theta(\theta) v(\theta, t) \\ &\quad - \left[V^\theta(x, \theta, t) + \Phi_p(\theta)^\top \Lambda \Phi_p^\theta(\theta) \right] \omega. \end{aligned} \quad (13)$$

From (11) we see that

$$v(\theta(t), t) \in \mathcal{N}(\Phi_p^\theta(\theta(t))) \quad \forall t \geq 0$$

ensures that the sign indefinite term $\Phi_p(\theta)^\top \Lambda \Phi_p^\theta(\theta) v(\theta, t)$ vanishes from (13). One way to achieve this is to let all speed assignments be equal and dependent only on time, i.e. $v_i(\theta_i, t) = v_s(t)$, $i = 1, \dots, r$. Various choices can be made depending on the shape and the parametrization of the path. If the path is parameterized in terms of e.g. path length, θ will have the unit ‘meter’, and a speed assignment will correspond directly to the speed of the vessel. In this case, a purely time-dependent speed assignment is very feasible.

Gradient update law: Consider the last sign indefinite term in (13) and notice that $V^\theta(x, \theta, t) + \Phi_p(\theta)^\top \Lambda \Phi_p^\theta(\theta) = V_s^\theta(x, \theta, t)$. Inspired by the gradient algorithm described in [1], we choose

$$\begin{aligned} \omega(x, \theta, t) &= \Gamma \left[V^\theta(x, \theta, t) + \Phi_p(\theta)^\top \Lambda \Phi_p^\theta(\theta) \right]^\top \\ &= \Gamma V_s^\theta(x, \theta, t), \end{aligned}$$

where $\Gamma = \text{diag}(\gamma_1, \dots, \gamma_r) > 0$ is a gain matrix. Hence, we have the following derivative of V_s along the solutions of the closed-loop system

$$\dot{V}_s \leq -z^\top Q z - V_s^\theta(x, \theta, t) \Gamma V_s^\theta(x, \theta, t)^\top. \quad (14)$$

The controller realization becomes

$$\dot{\theta} = v - \omega = v(\theta, t) - \Gamma V_s^\theta(x, \theta, t). \quad (15)$$

If we choose $\gamma_i = 0$, $i = 1, \dots, r$ not only would the vessels become decoupled, without any synchronization, but the dynamic part of the control law becomes $\dot{\theta} = v(\theta, t)$ which is equivalent to trajectory tracking, dependent only on time t . This will reduce performance, as the update law for $\dot{\theta}$ has no information about the states of the vessels.

In [5], the authors considers a tracking update law by choosing $\omega = 0 \Rightarrow \dot{\theta} = v(\theta, t)$. This solves the formation maneuvering problem (FMP), since the control design in [5] only depends on a single path variable. In our case this will solve the maneuvering problem for the individual ships, but not the FMP, since synchronization of the θ_i s is disabled.

Before we proceed, we need the following lemma:

Lemma 1: [6, Lemma 2] Given $\Phi_p(\theta) : \mathbb{R}^r \rightarrow \mathbb{R}^q$, let $\Psi(\theta) = \Phi_p^\theta(\theta)^\top \Lambda \Phi_p(\theta) \in \mathbb{R}^r$. Then $\Psi(\theta) = 0$ if and only if $\Phi_p(\theta) = 0$. For each pair $0 < \delta_0 < \Delta_0$ there exist $\delta_1, \Delta_1 > 0$ such that

$$\delta_0 \leq |\Phi_p(\theta)| \leq \Delta_0 \Rightarrow \delta_1 \leq |\Psi(\theta)| \leq \Delta_1.$$

We are now ready to state our result in the following theorem:

Theorem 1: The overall closed-loop formation maneuvering system

$$\begin{aligned} \dot{z} &= Fz + \Gamma V_s^\theta(x, \theta, t)^\top \\ \dot{\theta} &= v(\theta, t) - \Gamma V_s^\theta(x, \theta, t)^\top \end{aligned} \quad (16)$$

is forward complete and solves the formation maneuvering problem, i.e. the set

$$\mathcal{M} = \{(z, \theta, t) : z = 0, \Phi_p(\theta) = 0\}$$

is UGAS.

Proof: To check that the proposed speed assignment is satisfied in \mathcal{M} , we notice that for $\phi_i = 0 \quad \forall i$ and $z = 0$, $\Phi_p(\theta) = 0$ and $V^\theta(x, \theta, t) = 2z^\top P z^\theta = 0$. This implies that $(z, \theta, t) \in \mathcal{M} \Rightarrow \omega = 0$ as required. Let $Z := [z^\top, \Phi_p(\theta)^\top]^\top$. For the synchronization Lyapunov function (12), we have the bounds

$$\begin{aligned} p_1 |Z|^2 &\leq V_s \leq p_2 |Z|^2 \\ \dot{V}_s &\leq -q_m |z|^2 \end{aligned}$$

where $p_1 = \min(p_m, 0.5\lambda_m)$ and $p_2 = \max(p_M, 0.5\lambda_M)$. This implies that for all t in the maximal interval of definition $[0, T)$,

$$|Z(t)| \leq \sqrt{\frac{p_2}{p_1}} |Z(0)|.$$

Hence, by the assumed smoothness of the plant dynamics and boundedness of all path signals and speed assignment signals, implying that the right-hand side of (16) depends continuously on (θ, t) through bounded functions, and with z bounded, it follows that (16) is bounded on the maximal interval of definition. This excludes finite escape times so $T = \infty$. It is verified that $|(z, \theta, t)|_{\mathcal{M}} = |Z|$.

We now proceed by checking if there exists a positive definite function $\alpha_3 : R_{\geq 0} \rightarrow R_{\geq 0}$ such that $\dot{V}_s \leq -\alpha_3(|Z|)$. Consider (14), by setting $z = 0$ we see that $\dot{V}_s|_{z=0} = -\Psi(\theta)^\top \Lambda \Psi(\theta)$. By Lemma 1, we see that $\dot{V}_s = 0$ if and only if $Z = 0$. Otherwise, the r.h.s. of (14) is negative. With V_s radially unbounded and α_3 positive definite we can conclude, since the closed-loop is forward complete, that \mathcal{M} is UGAS. ■

A. Decentralized controller realization

Theorem 1 establishes that all path variables θ_i will become synchronized, so that the formation moves along the path in the desired setup. For a single vessel, the controller realizations (7), with gradient update law (15), are

$$\begin{aligned} u_i &= \alpha_{2i}(x_i, \theta_i, t) \\ \dot{\theta}_i &= v_i(\theta_i, t) \\ &\quad - \gamma_i \left\{ V_i^{\theta_i}(x_i, \theta_i, t) + \Phi_p^\theta(\theta)_i^\top \Lambda \Phi_p(\theta) \right\} \end{aligned} \quad (17)$$

where $\Phi_p^\theta(\theta)_i^\top$ is the i 'th row of $\Phi_p^\theta(\theta)^\top$.

Notice that the control laws only depend on the vessel's own states and the path variables θ_i from other vessels in the formation. From (17) it can be seen that $\Lambda = 0$ renders the update law for $\dot{\theta}_i$ identical to the dynamic update laws for maneuvering a single ship [2]. This choice of Λ decouples the vessels by disabling synchronization. On the other hand, in the limit as $\|\Lambda\| \rightarrow \infty$, the path variables will be identically synchronized at all times. As



Fig. 2. Cybership II

a result, this design generalizes maneuvering of ships with the extra feature of formation control

III. EXPERIMENTAL EVALUATION

As a demonstration of the proposed design procedure, a rendezvous maneuvering operation between Cybership II and a computer simulated ship was implemented and carried out in the Marine Cybernetics Laboratory (MCLab). This experiment can be thought of as an underway replenishment operation between the two ships.

We consider a dynamic ship model where the surge mode is decoupled from the sway and yaw mode. Subscript i denotes the i 'th ship. Let $\eta_i = [x_i, y_i, \psi_i]^\top$ be the earth fixed position vector, where (x_i, y_i) is the position on the ocean surface and ψ_i is the yaw angle (heading). Let $\nu_i = [u_i, v_i, r_i]^\top$ be the body-fixed velocity vector. The 3DOF equations of motion in surge, sway and yaw for a single ship are written

$$\dot{\eta}_i = R(\psi_i)\nu_i \quad (18a)$$

$$M_i\dot{\nu}_i + D_i\nu_i = \tau_i \quad (18b)$$

where $R(\psi_i) \in SO(3)$ is the rotation matrix, $M_i = M_i^\top > 0$ is the system inertia matrix including the hydrodynamic added inertia, D_i is the hydrodynamic damping matrix, and τ_i is the fully actuated vector of control forces. For more details regarding ship modelling, the reader is suggested to consult [7] and [8].

The desired path to be followed is given by $\xi_i(\theta_i) = [x_{id}(\theta_i), y_{id}(\theta_i), \psi_{id}(\theta_i)]^\top$ where θ_i is the parametrization variable and the desired heading is computed in (2). Let the speed assignment be $v_i(\theta, t)$ for each vessel. The maneuvering design yields the following signals for each

vessel

$$\begin{aligned} z_{1i} &:= \eta_i - \xi_i(\theta_i) \\ z_{2i} &:= \nu_i - \alpha_{1i} \\ \alpha_{1i} &= R(\psi_i)^\top \left[A_{1i}z_{1i} + \xi_i^{\theta_i}(\theta_i) v_i(\theta_i, t) \right] \\ \sigma_{1i} &= \dot{R}^\top R \alpha_{1i} + R^\top \left[A_{1i}R\nu_i + \xi_i^{\theta_i} v_i^t \right] \\ \alpha_{1i}^{\theta_i} &= R^\top \left[-A_{1i}\xi_i^{\theta_i} + \xi_i^{\theta_i^2} v_i + \xi_i^{\theta_i} v_i^{\theta_i} \right] \\ V_i^{\theta_i} &= -2z_{1i}^\top P_{1i} \xi_i^{\theta_i} - 2z_{2i}^\top P_{2i} \alpha_{1i}^{\theta_i}. \end{aligned}$$

Let $v_1 = v_2 = v_s = \text{constant}$ to ensure that $v(\theta, t) \in \mathcal{N}(\Phi_p^\theta(\theta)) \forall t \geq 0$. With the paths parametrized in terms of path length, the speed assignment for the FRP will be the same as a desired surge speed along the path.

Given the synchronization constraint function $\Phi_p(\theta)$ and the corresponding Jacobian, the control law for Vessel i is

$$\begin{aligned} \tau_i &= M_i[-P_{2i}^{-1}R(\psi_i)^\top P_{1i}z_{1i} + A_{2i}z_{2i} \\ &\quad + M_i^{-1}D_i\nu_i + \sigma_1 + \alpha_{1i}^{\theta_i}v_s] \quad (19) \end{aligned}$$

$$\dot{\theta}_i = v_s - \gamma_i \left[V_i^{\theta_i} + \Phi_p^\theta(\theta)_i^\top \Lambda \Phi_p(\theta) \right], \quad (20)$$

where $\Phi_p^\theta(\theta)_i^\top$ is the i 'th row of $\Phi_p^\theta(\theta)^\top$.

A. Setup

The MCLab is an experimental laboratory for testing scale models of ships, rigs, underwater vehicles and propulsion systems located at NTNU, Trondheim, Norway. It is a joint facility between Department of Engineering Cybernetics, Department of Marine Technology (NTNU), and Marintek.

The software is developed using rapid prototyping techniques, and automatic code generation with Matlab, Simulink, Real-Time Workshop, and Opal RT-Lab. The simulation software was developed on a host PC under RT-Lab, and executed on the vessel in the target PC which runs the QNX Neutrino Version 6.2 RT-OS. All control commands are transferred from the control room to the ship via a wireless communication link and the experimental results are presented in real-time on the host PC using LabVIEW as a graphical user interface (GUI). Among other things, the synchronization feature can be turned on and off during experiments. For more information on the experimental setup, see [9] and [10].

Cybership II (Fig. 2) is a scale-model (1:70) of an offshore supply vessel and is equipped with 2 rpm controlled propellers, 2 rudders and 1 bow thruster. The model ship has a mass of 23.8 kg and a length of 1.255 m. The control plant parameters are [11]:

$$\begin{aligned} M &= \begin{bmatrix} 23.8 & 0 & 0 \\ 0 & 33.8 & 1.0948 \\ 0 & 1.0948 & 2.764 \end{bmatrix}, \\ D &= \begin{bmatrix} 2 & 0 & 0 \\ 0 & 7 & 0.1 \\ 0 & 0.1 & 0.5 \end{bmatrix}. \end{aligned}$$

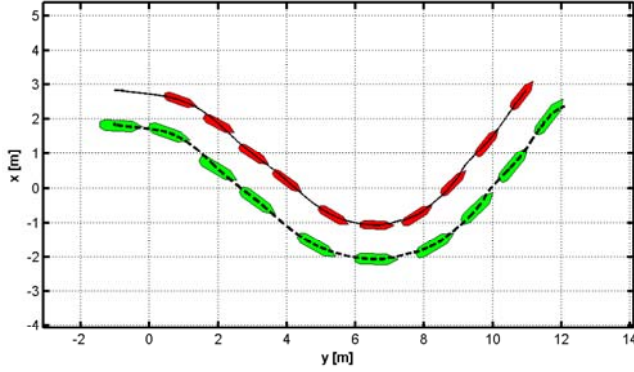


Fig. 3. Snapshots of Cybership II (- -) and the computer simulated ship (-) in the MCLab basin.

The smooth path for the Formation Reference Point is created using a path planner with a set of given waypoints in the MCLab basin. The designation vectors are $l_1 = [0, 0, 0]^T$ and $l_2 = [0, 1, 0]^T$ which means that the FRP coincide with Cybership II. The speed assignment is a desired surge speed, set by the operator using the GUI. The controller parameters are set as: $A_{1i} = \text{diag}(0.03, 0.03, 0.03)$, $A_{2i} = \text{diag}(2.5, 2.5, 2.5)$, $P_{1i} = \text{diag}(0.1, 0.1, 0.1)$, $P_{2I} = I_{3 \times 3}$, $\gamma_i = 0.15$, $\Lambda = \text{diag}(1.5, 1.5)$ and $p = 1$. The initial conditions are $\nu_1(0) = \nu_2(0) = [0, 0, 0]^T$, $\theta_1(0) = 0$ and $\theta_2(0) = 1$.

B. Experimental Results

The aim of the experiment is to verify the synchronization property of the extended maneuvering controller. Only the scalar path variables θ_1 and θ_2 are necessary to endure synchronization, hence only two signals are communicated during the experiment. The resulting position plot is seen in Fig. 3. The plot shows that the virtual ship starts ahead of Cybership II and that the two ships converge smoothly to their desired path. Until synchronization is turned on, the distance between the ships stays the same and the difference between the path variables θ_1 and θ_2 is almost constant.

After synchronization is enabled and has occurred about halfway through the simulation, the ships move on courses parallel to each other. In Fig. 4, the synchronization of the path variables can be seen for two different synchronization gains ($\Lambda = 1.5I$ and $\Lambda = I$). The difference between the two synchronization gains is reflected in the speed of the synchronization $|\theta_1 - \theta_2|$.

IV. CONCLUSION

We have shown that by constructing decentralized control laws that solves a maneuvering problem for the individual vessels and together ensure synchronization, efficient formation control of r systems can be achieved with a small amount of real-time communication. Model experiments demonstrate the performance of the proposed controller and clearly illustrates how the synchronization speed is set

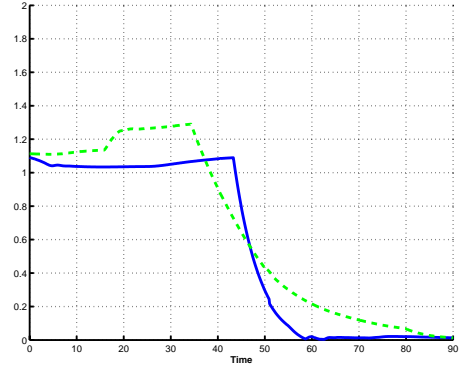


Fig. 4. Synchronization of the path variables θ_1 and θ_2 with two different synchronization gains, $\lambda_i = 1.5$ (-) and $\lambda_i = 1$ (- -).

by the weight matrix Λ . The only signals communicated between the virtual ship and Cybership II were the path variables. Compared to the results in [5] we have achieved new results on path following and formation control while reducing the amount of inter-vessel communication during the experiments.

REFERENCES

- [1] R. Skjetne, T. I. Fossen, and P. V. Kokotović, "Robust Output Maneuvering for a Class of Nonlinear Systems," *Automatica*, vol. 40, no. 3, pp. 373–383, 2004.
- [2] —, "Adaptive maneuvering with experiments for a model ship in a marine control laboratory," *Automatica*, 2004, provisionally accepted.
- [3] D. J. Stilwell and B. E. Bishop, "Platoons of Underwater Vehicles," *IEEE Control Systems Magazine*, vol. 20, no. 6, pp. 45–52, 2000.
- [4] D. A. Schoenwald, "Auvs: In space, air, water, and on the ground," *IEEE Control Systems Magazine*, vol. 20, no. 6, pp. 15–18, 2000.
- [5] R. Skjetne, S. Moi, and T. I. Fossen, "Nonlinear Formation Control of Marine Craft," in *Proc. 41st IEEE Conf. Decision and Control*. Las Vegas, Nevada, USA: IEEE, Dec. 10–13 2002, pp. 1699–1704.
- [6] R. Skjetne, I.-A. F. Ihle, and T. I. Fossen, "Formation Control by Synchronizing Multiple Maneuvering Systems," in *Proc. 6th IFAC Conference on Manoeuvring and Control of Marine Crafts*, Girona, Spain, Sep. 17–19 2003, pp. 280–285.
- [7] T. I. Fossen, *Marine Control Systems: Guidance, Navigation and Control of Ships, Rigs and Underwater Vehicles*. Trondheim: Marine Cybernetics, 2002, <<http://www.marinecybernetics.com>>.
- [8] T. I. Fossen and Ø. N. Smogeli, "Nonlinear time-domain strip theory formulation for low-speed maneuvering and station-keeping," *Modelling, Identification and Control*, vol. 25, no. 4, 2004.
- [9] I.-A. F. Ihle, "Observer design for synchronization of two vessels with unreliable position measurements," Master's thesis, Department of Engineering Cybernetics, Norwegian University of Science and Technology (NTNU), Trondheim, Norway, 2003.
- [10] J. Corneliussen, "Implementation of Guidance System for Cybership II," Master's thesis, Department of Engineering Cybernetics, Norwegian University of Science and Technology (NTNU), Trondheim, Norway, 2003.
- [11] K.-P. Lindegaard, "Acceleration Feedback in Dynamic Positioning," Ph.D. dissertation, Department of Engineering Cybernetics, Norwegian University of Science and Technology (NTNU), Trondheim, Norway, 2003.